Emergent swarming states in active particles system with opposite anisotropic interactions

Cite as: Chin. J. Chem. Phys. **33**, 717 (2020); https://doi.org/10.1063/1674-0068/cjcp2003037
Submitted: 24 March 2020 . Accepted: 07 April 2020 . Published Online: 21 January 2021

Yong-liang Gou, Hui-jun Jiang, and Zhong-huai Hou

ARTICLE

Emergent Swarming States in Active Particles System with Opposite Anisotropic Interactions

Yong-liang Gou, Hui-jun Jiang, Zhong-huai Hou*

Department of Chemical Physics & Hefei National Laboratory for Physical Sciences at the Microscale, iChEM, University of Science and Technology of China, Hefei 230026, China

(Dated: Received on March 24, 2020; Accepted on April 7, 2020)

From the organization of animal flocks to the emergence of swarming behaviors in bacterial suspension, populations of motile organisms at all scales display coherent collective motion. Recent studies showed that the anisotropic interaction between active particles plays a key role in the phase behaviors. Here we investigate the collective behaviors of based-active Janus particles that experience an anisotropic interaction of which the orientation is opposite to the direction of active force by using Langevin dynamics simulations in two dimensional space. Interestingly, the system shows emergence of collective swarming states upon increasing the total area fraction of particles, which is not observed in systems without anisotropic interaction or activity. The threshold for emergence of swarming states decreases as particle activity or interaction strength increases. We have also performed basic kinetic analysis to reproduce the essential features of the simulation results. Our results demonstrate that anisotropic interactions at the individual level are sufficient to set homogeneous active particles into stable directed motion.

Key words: Active particle, Anisotropic interaction, Swarming

I. INTRODUCTION

Collective behaviors of active matter have emerged at all scales in nature, from the animal flocks [1–3] to the emergence of unidirectional motion of bacteria [4, 5]. Understanding the physical origins of such collective behaviors is of great importance for revealing the mystery of living systems and further for manufacturing smart materials [6, 7]. One of the most popular models is Vicsek model [8], which considers self-propelled particles interacting solely via simple alignment rules. It has been proven that alignment rules at the individual level could account for the emergence of collective behaviors at the group level. Based on this model, many investigations [9–12] have been done and lots of interesting results were acquired. For instance, Tailleur *et al*. [9] investigated the behavior of interacting self-propulsion particles with density-dependent motility and found that interactions lead generically to the formation of host of patterns. Using Vicsek-style models with an Ornstein-Uhlenbeck process, Nagai *et al*. [10] showed that memory is a crucial ingredient for the collective properties of self-propelled particles and uncovered a rich variety of collective phases that were not observed in usual active systems, including vortex lattices and active foams.

To step further, more complex collective behaviors have been systematically found in experiments, including the formation of large-scale vortices [13] and swarming behaviors [14]. All these model systems rely on genuine physical interactions to generate collective motion. These interactions are complex and uncontrolled but decisive for the large-scale behavior of the populations. A fascinating issue is how to measure and describe these interactions theoretically. A prior work by Bricard *et al*. [15] pointed out that dilute populations of millions of colloidal rolling particles self-organize to achieve coherent motion in a unique direction. This is the first time for establishing the existence of a polar-liquid phase experimentally involving active materials. They demonstrated that genuine physical interactions at the individual level are sufficient to set homogeneous active populations into stable directed motion.

As mentioned above, the physical interactions among individuals play a key role and should be considered. Fortunately, advances in colloidal chemistry have led to the reliable synthesis of artificial active self-propelling colloids [16–19], in which the dynamics and interaction between particles can be better controlled to understand the physical origins of the emergent phenomena in active matter. Especially, many synthesized active particles are of Janus type [20–22], characterized by having two sides or at least two surfaces of different chemistry and/or polarity, wherein self-propulsion arises from non-uniform properties such as temperature [23], or chemical activity [24], from light-driving [25], or

*Author to whom correspondence should be addressed. E-mail: hzhlj@ustc.edu.cn

even from bubbles [26]. Interestingly, the interaction between these Janus particles can be strongly anisotropic, as suggested by Tarazona and co-workers [27] who specialized on amphiphilic particles composed of a hydrophilic and a hydrophobic hemispheres. However, in most previous works of active particles, such anisotropic Janus interactions have not been systematically accounted for. Therefore, an interesting question is what will happen if we consider the activity and anisotropic interaction simultaneously.

Actually, such an issue has raised increasing attention very recently [6]. Experimentally, Gao *et al.* [20] demonstrated that hydrophobic interactions provide a new approach for constructing defined assemblies of chemically powered Janus particle motors. Granick and co-workers [14] found that anisotropic interactions between active units can be controlled along with the activity simultaneously, consequently several interesting new dynamic phase states such as chains, rotating pinwheels were observed. On the simulation side, our recent work [28] showed that active Janus systems, in which self-propulsion force acts along the orientation of anisotropic interactions, can show interesting reentrance phase separation behaviors. Mallory *et al.* [29] studied the phenomenology of a two dimensional dilute suspension of active amphiphilic Janus particles which illustrate how the geometry of the colloids and the directionality of their interactions can be used to control the physical properties of the assembled active aggregates.

We have proposed general biased-active particle (BAP) model [30] very recently, wherein the direction of active force is not aligned with the anisotropic interaction orientation but has an angle θ in between. Remarkably, a highly ordered superlattice consisting of small hexagon clusters with dynamic chirality emerges within a proper range of active force, given that the biased angle is not too small in a mixture of biased-active and passive particles. In fact, such a model would provide a new "design" strategy for active particles system, offering a great opportunity to explore a variety of new fascinating collective behaviors. Since the angle θ could vary in $(0, \pi)$, a lot of interesting phase behaviors would be expected and many more systematic studies are demanded. Experimentally, the BAPs are easier to synthesize for the cases of θ=0 and π. Investigation of these system is more practical and instructive. Because the study of θ=0 has been done, in this work we want to know how would the Janus interactions affect the collective behaviors of active system if the directions of activity and anisotropic interaction are opposite to each other (θ=π).

Motivated by this, in this work, we have studied the collective behaviors in a system of active particles with opposite anisotropic interaction by using two-dimensional Langevin dynamics simulations. Each active particle i is of Janus type, and one can define an unit vector $\mathbf{q}_i$ as the orientation of the particle pointing

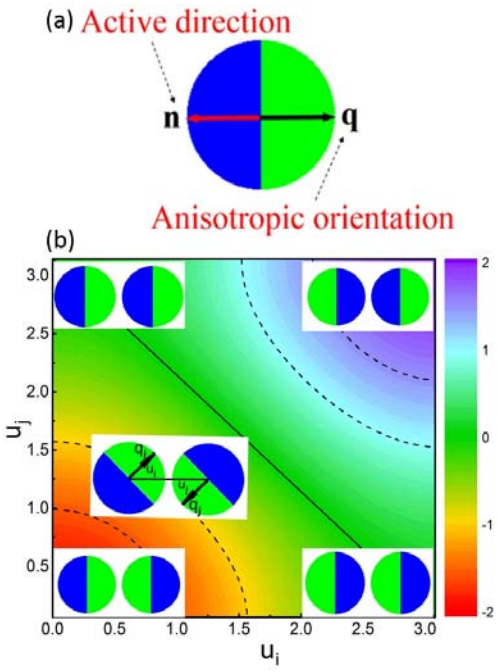

FIG. 1 (a) Schematic of active Janus particle with opposite direction of active force and orientation of anisotropic interaction. The green side(face) is attractive and the blue(tail) one is repulsive. **n** represents the active direction and **q** the anisotropic orientation. (b) Contour plot of Janus potential $U_{\rm AN}$ for C=1.0 and r_{ij}=1.0 in the u_i-u_j plane, wherein $u_{i(j)}$ is defined as the angle between vectors $\mathbf{q}_{i(j)}$ and $\mathbf{r}_{ij(ji)}$ as shown in the middle inset. The insets at the corners show pair configurations corresponding to the values of $u_{i(j)}$.

to the face (green) side as shown in FIG. 1(a), which is opposite to direction of the self-propulsion force denoted by $\mathbf{n}_i$. In particular, two particles i and j subjected to anisotropic interaction $U_{\rm AN}(r_{ij}, \mathbf{q}_i, \mathbf{q}_j)$, which is dependent on the distance r_{ij} and directions $\mathbf{q}_{i,j}$ with tunable strength given by C, such that the face (green) sides are mostly attractive while the back sides (blue) are repulsive. In another word, the active force tends to push two particles away from their attractive side. Interestingly, we find that there is an emergence of collective swarming behaviors within a proper range of active force and interaction strength: Upon increasing the area fraction ϕ to some threshold value $\phi_{\rm c}$, the system shows a clearcut transition from a homogenous disordered state to a directional swarming motion. Detailed simulations show that the critical value $\phi_{\rm c}$ decreases monotonically with both the active force amplitude $F_{\rm a}$ and the coupling strength C. We have also performed a kinetic analysis to illustrate the underlying mechanism of the formation of swarming band which can reproduce the essential features of the simulation results.

The remainder of the paper is organized as follows. In Section II, we give detailed descriptions of the model and simulation dynamics. Section III presents the main simulation results of the phase behaviors, particularly

DOI:10.1063/1674-0068/cjcp2003037

the emergence of swarming behavior. In Section IV, we try to give a basic kinetic analysis about how the swarming band is formed and how the critical value ϕ_c depends on system parameters, followed by discussions and conclusions in Section V.

II. MODEL

We consider a two-dimensional system containing N Janus disk particles of the same diameter σ with active force along direction $\mathbf{n}$ opposite to the face direction $\mathbf{q}$ as depicted in FIG. 1. The interaction U_{ij} between two particles i and j contains two terms,

$$U_{ij}(\mathbf{r}_{ij},\mathbf{q}_i,\mathbf{q}_j)=U_{\mathrm{WCA}}(r_{ij})+U_{\mathrm{AN}}(\mathbf{r}_{ij},\mathbf{q}_i,\mathbf{q}_j) \quad (1)$$

where $\mathbf{r}_{ij}$=$\mathbf{r}_j-\mathbf{r}_i$ is the vector pointing from particles i to j, and r_{ij}=$|\mathbf{r}_{ij}|$ is the corresponding distance. The first term $U_{\mathrm{WCA}}(r_{ij})$ denotes an isotropic excluded volume interaction given by the WCA potential [31],

$$U_{\mathrm{WCA}}(r_{ij})=4\varepsilon\left[\left(\frac{\sigma}{r_{ij}}\right)^{12}-\left(\frac{\sigma}{r_{ij}}\right)^{6}\right] \quad (2)$$

if r_{ij}<$2^{1/6}\sigma$ and zero otherwise, with ε the interaction strength. The second term $U_{\mathrm{AN}}(\mathbf{r}_{ij},\mathbf{q}_i,\mathbf{q}_j)$ is the anisotropic Yukawa interaction potential whose form is given by [32, 33]

$$U_{\mathrm{AN}}(\mathbf{r}_{ij},\mathbf{q}_i,\mathbf{q}_j)=\frac{C\mathrm{e}^{-\lambda(r_{ij}-\sigma)}}{r_{ij}^2}(\mathbf{q}_i-\mathbf{q}_j)\cdot\mathbf{r}_{ji} \quad (3)$$

where C denotes the Janus interaction strength and λ denotes the characteristic interaction length. In FIG. 1(b), the contour plot of Janus potential U_{AN} in the u_i-u_j plane, wherein $u_{i(j)}$ is the angle between vectors $\mathbf{q}_{i(j)}$ and $\mathbf{r}_{ij(ji)}$ as shown in the inset of FIG. 1(b). For a fixed particle distance, the configuration with u_i=u_j=0 (face-to-face) locates at the energy minimum, while that with u_i=u_j=π (tail-to-tail) configuration is at the energy maximum. So the Janus interaction is attractive (repulsive) for configuration of face-to-face (tail-to-tail). For the face-to-tail configuration, there is no Janus interaction between particles.

The dynamic equation governing the evolution of $\mathbf{r}_i$ (i=$1,2,...,N$) is then given by

$$\dot{\mathbf{r}}_i=\frac{D_{\mathrm{t}}}{k_{\mathrm{B}}T}\left(-\sum_{j\neq i}^{N}\frac{\partial U_{ij}}{\partial\mathbf{r}_i}+F_{\mathrm{a}}\mathbf{n}_i\right)+\boldsymbol{\xi}_i \quad (4)$$

where k_{B} denotes the Boltzmann constant, T is the temperature, and $\boldsymbol{\xi}_i$ is the thermal fluctuation satisfying fluctuation-dissipation relationship $\langle\boldsymbol{\xi}_i(t)\boldsymbol{\xi}_j(t')\rangle$=$2D_{\mathrm{t}}\mathbf{1}\delta_{ij}\delta(t-t')$ with D_{t} the translational diffusion coefficient and $\mathbf{1}$ the unit tensor. F_{a} is the magnitude of the active force which in the absence of interactions, will move a particle with speed v_p=$D_{\mathrm{t}}F_{\mathrm{a}}/k_{\mathrm{B}}T$.

Similar to conventional active Brownian particles, the direction of active force $\mathbf{n}_i$ (and thus $\mathbf{q}_i$) changes via random rotational diffusion. In addition, the anisotropic interaction also exerts a torque on the particle and thus also leads to the change of orientation $\mathbf{q}_i$. Therefore, the dynamic equations of $\mathbf{q}_i$ can be written as,

$$\dot{\mathbf{q}}_i=-\frac{D_{\mathrm{r}}}{k_{\mathrm{B}}T}\sum_{j\neq i}^{N}\frac{\partial U_{\mathrm{AN}}(\mathbf{r}_{ij},\mathbf{q}_i,\mathbf{q}_j)}{\partial\omega_i}\left(\frac{\partial\mathbf{q}_{\mathrm{i}}}{\partial\omega_i}\right)+\boldsymbol{\eta}_i\times\mathbf{q}_i \quad (5)$$

wherein ω_i is the angle between $\mathbf{q}_i$ and the x-axis, *i.e.*, $\mathbf{q}_i$=$(\cos\omega_i,\sin\omega_i)$. This equation is obtained via $\mathrm{d}\mathbf{q}_i/\mathrm{d}t=(\partial\mathbf{q}_i/\partial\omega_i)(\mathrm{d}\omega_i/\mathrm{d}t)$, wherein

$$\frac{\mathrm{d}\omega_i}{\mathrm{d}t}=-\left(\frac{D_{\mathrm{r}}}{k_{\mathrm{B}}T}\right)\left(\frac{\partial U_i}{\partial\omega_i}\right)+\sqrt{2D_{\mathrm{r}}}\eta_\omega(t) \quad (6)$$

with U_i the total force subjected by particle i, D_{r} the rotational diffusion coefficient and $\eta_\omega(t)$ a Gaussian white noise with zero variance and unit variance. Since U_{WCA} is isotropic, we have

$$\frac{\partial U_i}{\partial\omega_i}=\frac{\sum_{j\neq i}^{N}\partial U_{\mathrm{AN}}(\mathbf{r}_{ij},\mathbf{q}_i,\mathbf{q}_j)}{\partial\omega_i} \quad (7)$$

thus obtaining the first deterministic term in Eq.(5). The noise term for $\dot{\mathbf{q}}_i$ is $(\partial\mathbf{q}_i/\partial\omega_i)\sqrt{2D_r}\eta_\omega(t)$ which is actually a noise vector perpendicular to $\mathbf{q}_i$ and can be written as $\boldsymbol{\eta}_i\times\mathbf{q}_i$, where $\boldsymbol{\eta}_i$ is a noise vector satisfying $\langle\boldsymbol{\eta}_i(t)\boldsymbol{\eta}_j(t')\rangle$=$2D_r\mathbf{1}\delta_{ij}\delta(t-t')$. In numerics, we actually calculate the evolution of θ_i via Eq.(6). Note that the rotational and translational diffusion coefficients are couples via D_{r}=$3D_{\mathrm{t}}/\sigma^2$ in our work.

Simulations are performed in a $L\times L$ (L changes with area fraction ϕ) two dimensional square box with periodic boundary conditions. σ, $k_{\mathrm{B}}T$, and τ=σ^2/D_{t} are chosen as the dimensionless units for length, energy and time, respectively. We fix ε=1.0, λ=$3\sigma^{-1}$ and N=10084 during the simulations if not otherwise stated. The system is parameterized by three dimensionless values, the area fraction ϕ=$N\pi\sigma^2/4L^2$, Péclet number Pe=$v_p\tau/\sigma$ and anisotropic interaction strength C. The simulation time step is Δt=$10^{-4}\tau$ and all simulations start from random initial conditions and run for long enough time to ensure the system has reached the stationary state.

III. PHASE BEHAVIORS

To begin with, we investigate how the collective behavior of active Janus particles depends on the area fraction ϕ with fixed Péclet number Pe and interaction strength C. FIG. 2 shows the results for Pe=360 and C=9. At low area fraction, the particles form an isotropic disordered state, wherein all particles move in random directions as shown in FIG. 2(a) for ϕ=0.1.

DOI:10.1063/1674-0068/cjcp2003037

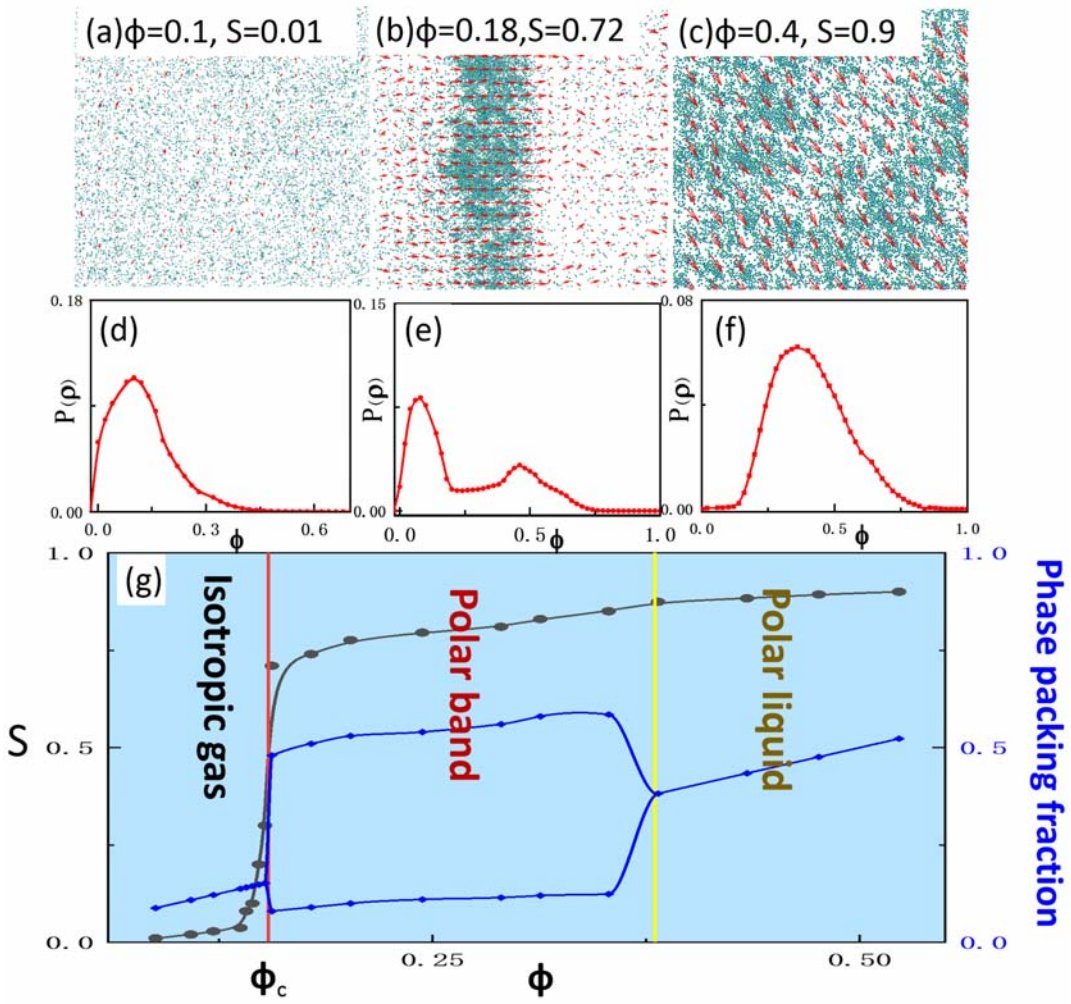

FIG. 2 Typical phase behaviors for active particles with opposite Janus interaction under fixed Pe=360 and C=9. (a) Isotropic gas, ϕ=0.1. (b) Polar band, ϕ=0.18. (c) Homogeneous polar liquid, ϕ=0.4. The red arrows in (a−c) represent the local polar order magnitude and its directions. Panels (d−f) show the corresponding density distributions. (g) Left axis: global polar order S as a function of ϕ (black line). Right axis: Phase densities as a function of area fraction (blue line). Swarming polar band occurs as ϕ exceeds ϕ_c=0.15, and ϕ_c is dependent on C and Pe.

The system is homogeneous, and the probability distribution function (PDF) for density shows a single peak as depicted in FIG. 2(d). Upon increasing ϕ to a larger value, say ϕ=0.18 as shown in FIG. 2(b), interestingly, we observe a clearcut phase separated behavior wherein the system contains a dense band immersed in a dilute 'gas' phase. Moreover, the band shows swarming behavior, *i.e.*, all the particles move in nearly the same direction. Accordingly, the density distribution of the system is depicted in FIG. 2(e), which contains two peaks, one at $\phi\approx$0.54 corresponding to the dense swarming band and the other at $\phi\approx$0.1 corresponding to the dilute gas phase. If the area fraction is too large, for instance ϕ=0.4 as shown in FIG. 2(c), the swarming band may span over all the box and no phase separation occurs any more. In this case, all the particles move in the same direction (which could be random) forming a polar liquid phase. Accordingly, the density distribution function becomes single-peaked again as shown in FIG. 2(f).

To quantitatively describe the swarm behavior, it is convenient to introduce the polarization order parameter $S=\left\langle \frac{1}{N}\sum_{i=1}^{N}\cos(\mathbf{n_i}-\bar{\mathbf{n}})\right\rangle$, where $\bar{\mathbf{n}}$ represents the average orientation of all particles and $\langle\rangle$ denotes average over ensemble and time. For a perfect swarm state where all particles move in the same direction, S=1, and S=0 for disordered gas phase. In FIG. 2(g), the dependence of S (black line) in the area fraction ϕ is shown for Pe=360 and C=9. Clearly, a sharp transition takes place at $\phi_c\approx$0.15 where S changes abruptly from nearly zero to about 0.75 in a vary narrow range of ϕ, followed by a slow increase of S to nearly 0.9 with increment of ϕ. It is also possible to define a local polar order parameter $\bar{S}_i$ which represents the local area order and is the

DOI:10.1063/1674-0068/cjcp2003037

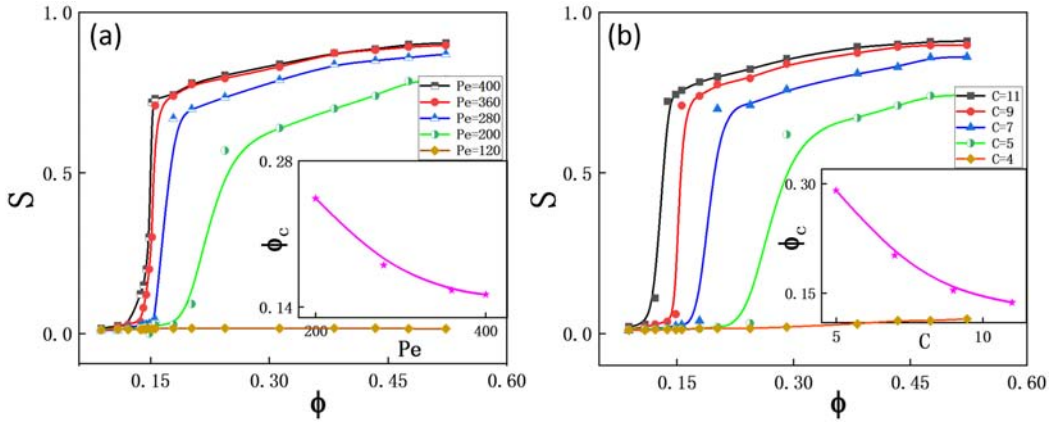

FIG. 3 (a) The effect of different Pe =400, 360, 280, 200, 120 under fixed C=9 for the emergent swarming behavior. The inset graph represents the relationship between Pe and critical area fraction ϕ_c. (b) The effect of different C=11, 9, 7, 5, 4 under fixed Pe=360 on the emergent swarming behavior. The inset graph represents the relationship between C and critical area fraction ϕ_c.

averaged value of $\cos(\mathbf{n}_j - \overline{\mathbf{n}})$ over the particles j contained in the corresponding region. In FIG. 2(a−c), we draw $\bar{S}_i$ by small red arrows, where the length denotes its amplitude and the direction represents the averaged particle orientation within the local range.

Note that the variation of S does not reflect the change from phase-separated swarming state in FIG. 2(b) to homogeneous polar liquid state in FIG. 2(c). Therefore, we have also drawn the dependence of phase packing fraction on ϕ as shown by the blue lines in FIG. 2(g). Within the range $\phi\in(\phi_c, \phi_1)$, where $\phi_1\approx0.36$ corresponds to the transition from swarming band to polar liquid, the phase packing fraction shows two clearcut branches, one to the dense swarming phase and the other to the gas phase. It is interesting to note that the area fraction of dense band keeps almost the same ($\phi_{\rm dense}\approx0.56$) within this phase-separated range of ϕ, until the band spans over the whole system and the phase separation disappears.

Above observations clearly demonstrate the emergence of collective swarming behavior of active Janus particles with increasing area fraction. Note that this is quite different from the well-known motility-induced phase separation (MIPS) of active Brownian particles, wherein the interaction among particles is isotropically pure-repulsive, such as those described by the WCA potentials. It is shown that for MIPS to happen, both the Péclet number and area fraction must be larger than some threshold values. In particular, no MIPS can be observed for ϕ<0.3, which is much larger than the critical value ϕ_c (0.15) here. Therefore, although the swarming state observed here is also a phase-separated state, obviously the anisotropic interaction has made the phase separation easier. Furthermore, area fraction of the dense swarming band is also much smaller than the dense cluster in MIPS, wherein the former is about 0.56 as shown in FIG. 2(g) while the latter is about the close-packed value $\phi_{\rm cp}=\pi/2\sqrt{3}$. Surely there exists no polar order in MIPS wherein the orientation of the particles is random and isotropic.

Comparison between the swarming behavior observed here and the usual MIPS clearly indicates the important role played in the anisotropic interaction. It is thus quite straightforward to ask how the above observations depend on the coupling strength C as well as the Péclet number Pe. The results are shown in FIG. 3. In FIG. 3(a), the order parameter S is presented as a function of ϕ for fixed C=9 but different values of Pe vary from 120 to 400. One can see that the curve shifts to larger values of ϕ with decreasing Pe, indicating that the critical value ϕ_c increases with decreasing Pe. If Pe is too small, say Pe=120, the value of S keeps nearly zero with increasing ϕ and no transition to swarming band behavior can be observed. Therefore, for a fixed interaction strength, there exists a threshold value for Pe below which no swarming behavior can be observed. Similarly in FIG. 3(b), the dependence of S on ϕ for fixed Pe=360 but varying C is presented. With increasing C, the curve also shifts to larger ϕ, indicating that ϕ_c also increases with decreasing interaction strength C. If C is too small as shown for C=4 in FIG. 3(b), no transition to swarming behavior can be observed.

With the variation of Pe or C, we see that the change of order parameter S becomes more and more continuous. To determine the transition point ϕ_c from disordered state to swarming band more accurately, we need to investigate PDFs of the density, as we have done to obtain FIG. 2 (d) to (f). With the variation of ϕ, the PDF changes from single-peaked to bimodal at the transition point ϕ_c. In FIG. 4, dependences of the (local) packing density on the total area fraction ϕ are shown for FIG. 4(a) fixed Pe=360 with varying C and FIG. 4(c) fixed C=9 with varying Pe. Transitions from homogeneous state to phase-separated swarming state are clearly demonstrated via the branching of packing density. Obviously, the transition point ϕ_c shifts to

DOI:10.1063/1674-0068/cjcp2003037

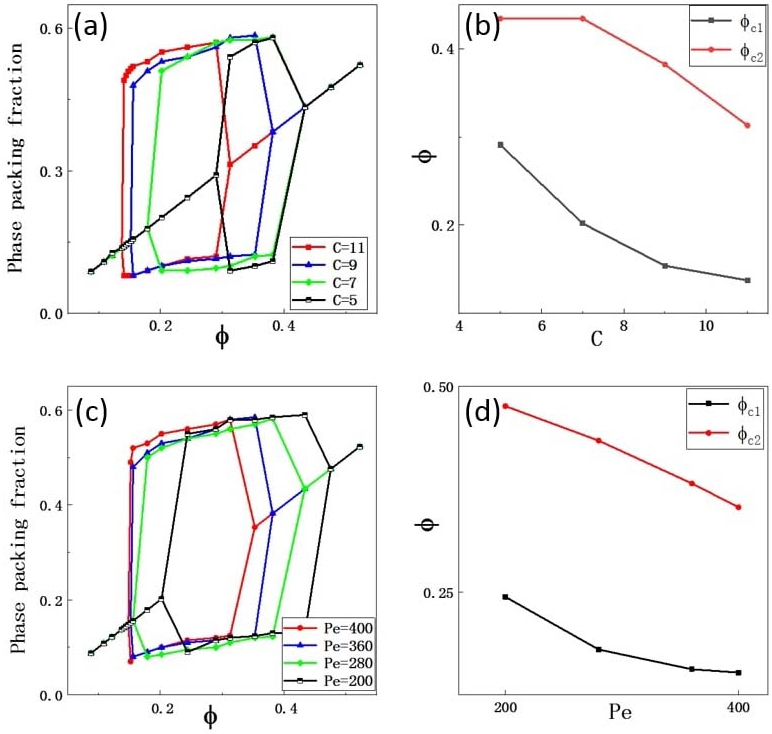

FIG. 4 The packing fraction of the swarming band (upper branch) and the disordered phase (lower branch) as functions of ϕ for (a) varying C with fixed Pe=360 and (c) varying Pe with fixed C=9. (b) and (d) illustrate the dependences of ϕ_{c1} and ϕ_{c2} on the $C(Pe)$ for fixed $Pe(C)$ respectively.

smaller values with increasing Pe or C, in accordance with the variation of S as expected. Also we can see that the system would finally change to the homogeneous polar liquid state if ϕ is larger than some threshold value similar to that observed in FIG.2(c). Similarly, this second transition point ϕ_{c2} also decreases with increasing Pe or C. The range $\phi\in(\phi_{c1},\phi_{c2})$ (ϕ_{c1}=ϕ_c) corresponds to where the phase-separated swarming band is observed. In FIG. 4 (b) and (d), the dependences of $\phi_{c1}(\phi_{c2})$ on $C(Pe)$ are presented for fixed $Pe(C)$ respectively, both showing monotonic decreasing tendency. It can be seen that the range of ϕ for swarming to occur is the largest for some intermediate values of Pe or C. Another interesting point to note that the density of the swarming band keeps nearly unchanged for different Pe or C, although it slightly increases with ϕ.

To get a global picture, we have depicted the contour plots of S in the parameter plane of (Pe,ϕ) as well as (Pe,C) in FIG. 5 (a) and (b), respectively. Also shown are the lines representing ϕ_{c1} (black) and ϕ_{c2} (blue). The plots clearly demonstrate that the polar band can only be observed when Pe and ϕ exceed some threshold values for given coupling strength C or when Pe and ϕ exceed some threshold values for given C. We note that the transition line of ϕ_{c1} does not coincide with the boundary for S=0, since already some polar order appears (S>0) before the band forms. Generally, the system is disordered and homogeneous for small packing fraction ϕ and small activity Pe (or interaction strength C), changes to collective swarming band in a range of the parameter plane with intermediate values of ϕ and Pe (or C), and further undergoes transition to homogeneous polar liquid in the upper-right corner of the parameter plane with too large ϕ and Pe (or C). Interestingly, by extension simulations, we find the swarming phenomena can still be observed in the range of $\theta\in(0.8\pi,\pi)$. In this range of biased angle, active Janus particles could be regarded as active repulsive particles if the activity is large enough, of which repulsive interactions could induce the alignment of particles. Besides, we also study how the system size would influence the global polar order (keeping the same area fraction). We find that the system size has nearly no influence on the global polar order and the critical value. Therefore, we conclude that the swarming behavior is robust with the change of system size.

IV. KINETIC ANALYSIS

The above observations clearly demonstrate the important roles played by the anisotropic interaction in the collective behaviors of active particles systems. As we already discussed, the emergent swarming behavior is quite different in phenomenon from the well-known MIPS which has already been thoroughly investigated in the past few years [34–37]. In particular, MIPS of simple active Brownian particles (ABPs) can be under-

DOI:10.1063/1674-0068/cjcp2003037

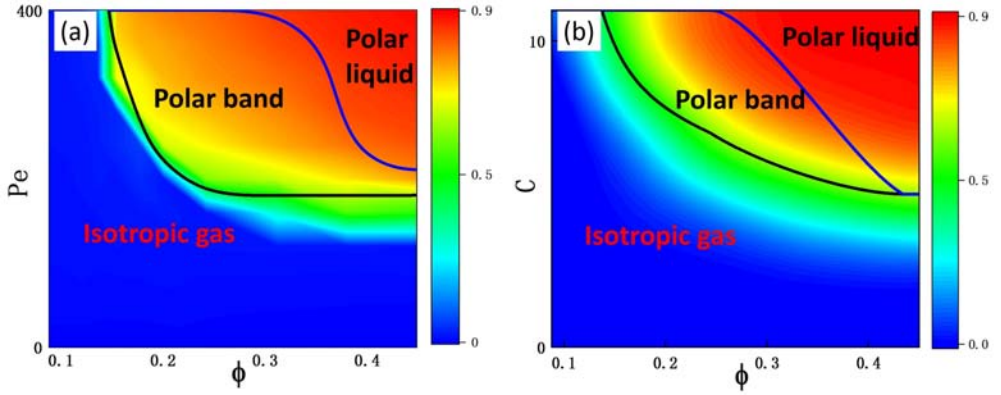

FIG. 5 (a) The phase diagram and contour plot of global polar order parameter S on the Pe-ϕ plane for C=9. (b) The phase diagram and contour plot of global polar order parameter S on the C-ϕ plane for Pe=360.

stood via a kinetic analysis [35, 38]. A cluster grows when ABPs pump into its surface due to active motion, while it shrinks when particles leave via random rotation. Qualitatively, assuming random orientation distribution in the gas phase and flat surface of the largest cluster, the flux for cluster growth, $k_{\rm in}$, is proportional to $\rho_{\rm g}v_p$ where v_p=$D_{\rm t}F_{\rm a}/k_{\rm B}T$ and $\rho_{\rm g}$ is the number density in the gas phase, the flux for cluster shrink, $k_{\rm out}$, can be estimated by $D_{\rm r}/\sigma$. Such a kinetic analysis is also applied to ABPs with isotropic long-range interactions to account for the reentrant phase behavior observed in simulations, and can also be used to obtain an effective free-energy landscape for the nucleation process.

Compared to the ABPs system, we have introduced an additional anisotropic interaction described by $U_{\rm AN}$. An important feature is that the direction of active force points to the 'back' side of the particle, *i.e.*, the repulsive side. Therefore, if two particles move toward each other, the effect of the Janus interaction is to repel them and make the particle change direction. This could lead to some kind of alignment effect, which is required by the emergence of swarming behavior. Another effect of the Janus interaction is that the particle orientation would no longer undergo random diffusion because of the torque, which could influence $k_{\rm out}$ for particle leaving an existing cluster or the swarming band.

In the present section, we try to perform a basic kinetic analysis to understand the formation of swarming band and some essential features of the phase behavior. To this end, we assume that in the steady state the band moving in the x-direction with a collective velocity $v_b \lesssim v_p$, with the surface particles all facing the left. Consider a tagged particle 1 with position $\mathbf{r}_1$=$(R,0)$ in front of the band with moving direction $\mathbf{n_a}$=$(\cos\theta,\sin\theta)$, where R is the distance to the surface and θ is the angle with the x-axis (see FIG. 6). For symmetric reasoning, we only need to investigate the case $\theta\in(0,\pi)$. For this particle, $\mathbf{q}_1$=$(-\cos\theta,-\sin\theta)$ pointing to the back-bottom direction. Consider another particle on the surface with position $\mathbf{r}_2$=$(0,y)$, of which the orientation is given by $\mathbf{q}_2$=$(-1,0)$ (the particle 2 shown in FIG. 6 has y=0). The anisotropic interaction between particles 1 and 2 is then given by

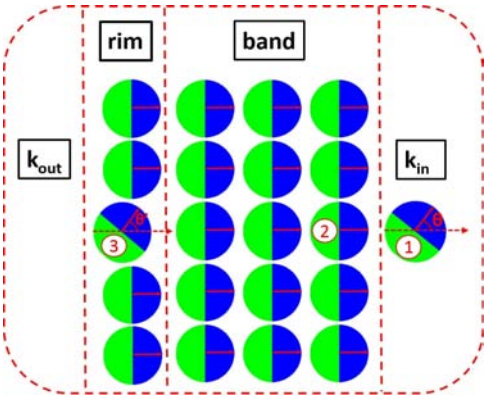

FIG. 6 Schematic representation of the swarming kinetics. The particle 1 in front of the band tends to align with the swarming direction (θ tends to decrease to zero) thus contributing to flux into the band. Particle 3 in the back surface will drift out the band if the angle θ' is larger than some threshold value and thus contributes to flux out of the band. See the main text.

$$V_{12}(y,\theta) = \frac{C\mathrm{e}^{-\lambda\sigma}\mathrm{e}^{-\lambda\left(y^2+R^2\right)^{1/2}}}{\left(y^2+R^2\right)^{1/2}}(\mathbf{q}_1-\mathbf{q}_2)\cdot\hat{\mathbf{r}}_{21} = \frac{C\mathrm{e}^{-\lambda\sigma}\mathrm{e}^{-\lambda\left(y^2+R^2\right)^{1/2}}}{\left(y^2+R^2\right)^{1/2}}\left[(1-\cos\theta)R+y\sin\theta\right]$$

The total interaction exerted by the surface particles on particle 1 would be approximately

$$V_1(R,\theta) = \int_{-L/2}^{L/2} V_{12}(y,\theta)\,\mathrm{d}y = Cf(R)(1-\cos\theta) \quad (8)$$

$$f(R) \equiv \int_{-L/2}^{L/2} \mathrm{e}^{-\lambda\sigma}R\mathrm{e}^{-\lambda\left(y^2+R^2\right)^{1/2}}/\left(y^2+R^2\right)\mathrm{d}y \quad (9)$$

DOI:10.1063/1674-0068/cjcp2003037

Eq.(9) is a function of R only in the limit of large L. One may further consider the particles in other layers of the band, which would lead to larger $f(R)$ but with same dependence on θ.

Under this interaction, the dynamic equation governing the change of orientation θ of particle 1 is given by (ignoring the WCA potential since it is reasonable to assume $R>R_c$ and the WCA potential does not take effect),

$$\begin{aligned}\frac{\mathrm{d}\theta}{\mathrm{d}t} &= -\beta D_r \partial_\theta V_1(R,\theta) + \sqrt{2D_r}\eta(\mathrm{t}) \\ &= -\beta D_r C f(R)\sin\theta + \sqrt{2D_r}\eta(t) \end{aligned} \tag{10}$$

Clearly, since $\sin\theta>0$ for $\theta\in(0,\pi)$, the angle θ experiences a restoring force to $\theta=0$, namely, the particles tend to align to the moving direction (with fluctuations). The alignment effect becomes stronger for larger Janus interaction strength. Therefore, for particles in front of the swarming band, anisotropic interactions make them align with the swarming direction.

Since the band moves to the right with nearly a constant velocity v_b, all the front particles with $v_p\cos\theta \leq v_b$ would finally join the band. Under the anisotropic interaction as discussed above, they will finally align with the band particles and move to the right with v_b. The flux k_{in} per unit length for the band to grow can then be estimated by

$$k_{\mathrm{in}} = \int_{\cos\theta\leq v_b/v_p} f(\theta)\left(v_b - v_p\cos\theta\right)\rho_{\mathrm{g}}\mathrm{d}\theta \tag{11}$$

where ρ_{g} and $f(\theta)$ are the number density and distribution of orientation in the low density gas phase, respectively. Before collision into the band, particles in the gas phase are isotropic in orientation, *i.e.*, $f(\theta)\approx 1/2\pi$. Note that $v_b=0$ corresponds to a static cluster, leading to $k_{\mathrm{in}}=\int_{\pi/2}^{3\pi/2} -f(\theta)\,v_p\cos\theta\mathrm{d}\theta=\rho_{\mathrm{g}}v_p/\pi$ in consistence with the flux for growth k_{in} in MIPS. For $v_b\neq 0$ here, one can obtain

$$k_{\mathrm{in}} \approx \rho_{\mathrm{g}}v_b\left[1-\pi^{-1}\cos^{-1}\frac{v_b}{v_p}\right] + 2\rho_{\mathrm{g}}v_p\left[1-\left(\frac{v_b}{v_p}\right)^2\right] \tag{12}$$

According to the simulation, v_b is slightly smaller than v_p, and v_b/v_p approaches 1 with increasing v_p. Using rough approximation 1 would lead to $k_{\mathrm{in}}\approx\rho_g v_p$. Generally, k_{in} increases with v_p such that the band is easier to form for larger v_p.

We now consider a particle 3 on the back surface of the band with orientation $\mathbf{q}_3=(-\cos\theta', -\sin\theta')$. Using similar analysis, we can obtain the interaction of particle 3 with the band particles in the second layer to the back as $V_3(R,\theta')=-Cf(R)(1-\cos\theta')$, where R is the distance between particle 3 and the second layer and $f(R)$ has the same functional form as mentioned before. Therefore, $\mathrm{d}\theta'/\mathrm{d}t=+\beta D_{\mathrm{r}} f(R)\sin\theta'+\sqrt{2D_{\mathrm{r}}}\eta(t)$ such that θ' tends to increase for $\theta'\in(0,\pi)$ or decrease for $\theta'\in(-\pi,0)$, indicating that its state with $\theta'=0$ is not stable against random rotation. If θ' exceeds some threshold values, the velocity in the x-direction of particle 3 would become too small to follow v_b, such that it tends to leave the band from behind. Note that $V_3(R,\theta')<0$, indicating that the particle 3 is adsorbed by the band. The velocity of particle 3 in x-direction can be estimated as $u_{3x}=v_p\cos\theta'+\beta D_t\left[-\partial_{r_{3x}}V_3(R,\theta')\right]=v_p\cos\theta'+C\kappa_1(1-\cos\theta')$, where r_{3x} is the x-component of $\mathbf{r}_3$ and fact has been used that $\partial_{r_{3x}}V_3=-\partial_R V_3$, and $\kappa_1=-\beta D_t\partial_R f(R)>0$ is introduced for shorthand notation. The particle would leave the band if $u_{3x}<v_b$, *i.e.*, $\cos\theta'<(v_b-C\kappa_1)/(v_p-C\kappa_1)$ defining a so-called escape cone $\theta'\in(\alpha,2\pi-\alpha)$, where $\alpha=\cos^{-1}(v_b-C\kappa_1)/(v_p-C\kappa_1)$. Therefore, the flux out the band (per unit length) can be calculated as

$$k_{\mathrm{out}} = \kappa_2\int_{\theta'\in(\alpha,2\pi-\alpha)}\left(v_b-u_{3x}\right)\rho_b p(\theta')\,\mathrm{d}\theta' \tag{13}$$

where κ_2 is a fitting parameter to account for other modifications [38], ρ_b is the number density of the swarming band and $p(\theta')$ is the stationary distribution of the orientation θ' on the back surface of the band. Clearly, if C is larger (stronger Janus interaction), α would be larger and the particles are harder to leave, indicating that k_{out} is smaller which is more favorable for the stability of the band. We note that this mechanism of flux out the band is quite different from that of MIPS, wherein the flux out of the static cluster is mainly by random rotation and the particles in a static cluster will leave the surface if its orientation points out of the cluster such that k_{out} is given by D_{r}/σ. In the swarming situation discussed here, the flux out of the band is mainly contributed by drift.

For a steady swarming band, equating k_{in} and k_{out} would yield a condition to solve the density ρ_{g}, which is dependent on v_p and C in a complicated manner. The simple criteria, that the fraction of particles in the gas phase would be less than one (such that high density band must be formed), give that $\phi_{\mathrm{c}}\geq\rho_g s_0$ allowing us to decide the critical fraction ϕ_c for band formation, where $s_0=\pi\sigma^2/4$ is the area of a single particle. Generally, it is easier for the band to form if k_{in} is larger or k_{out} is smaller, such that ϕ_{c} would be smaller. According to the analysis above, increasing activity v_p would increase k_{in}, while increasing Janus interaction C would reduce k_{out}, indicating that ϕ_{c} would decrease with both v_p and C, in qualitative agreement with the simulation results shown in FIG. 3.

To obtain quantitative results, however, one must know details about ρ_b and the distribution $p(\theta')$ in Eq.(13), which may also depend on v_p and C. According to the simulation results shown in FIG. 4, ρ_b is not sensitive to v_p and C, and can thus be viewed as a constant. Nevertheless, $p(\theta')$ is not easy to calculate theoretically. In the inset graph of FIG. 7, we have

DOI:10.1063/1674-0068/cjcp2003037

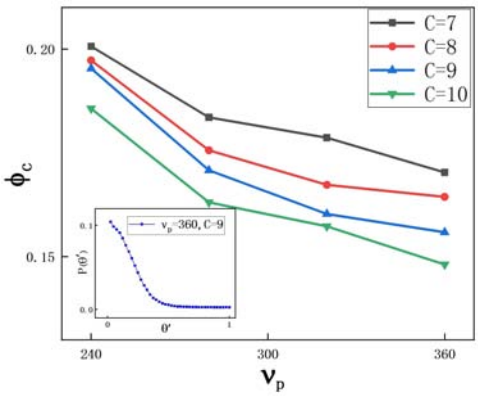

FIG. 7 Relationships between critical area fraction ϕ_c and activity v_p (equals to Pe in value) for different anisotropic interaction strength C, predicted by our kinetic model with fitting parameters κ_1=1, κ_2=28. The curves reproduce the essential features of the simulation observations, *i.e.*, ϕ_c decreases monotonically with both C and v_p. The inset graph shows an example of the stationary distribution of θ' on back surface of the band for fixed parameters of v_p=360 and C=9.

drawn the distribution $p(\theta')$ on the back layer of the band, obtained by direct simulations for fixed values of Janus strength C=9 and activity v_p=360. As can be seen, the distribution peaks at $\theta'\approx 0$ mainly stay in the range $(0, \pi/2)$. This distribution supports the picture that the particles leave the band via drift rather than random rotation. Substituting these simulated data for $p(\theta')$ into Eq.(13), we can then obtain $k_{\rm out}$, and thus ϕ_c by equating $k_{\rm in}$ and $k_{\rm out}$. Finally, we can obtain the dependence of ϕ_c on C and v_p with reasonable parameters as depicted in FIG. 7. Clearly, the theoretical analysis can reproduce the essential features of the simulation results, *i.e.*, ϕ_c decreases monotonically with C or v_p.

V. DISCUSSION AND CONCLUSION

In the literatures, there have been a few studies on the swarming behaviors of active systems, both theoretically and experimentally [8, 9, 13, 14, 39, 40]. The key factor that leads to directional swarming is the alignment of neighboring particles. Such alignment can result from a simple rule such as that in the pioneer Vicsek model, or caused by repulsion of particles and collisions. In our system, the formation of swarming also results from particle alignment as investigated in detail in Section IV. The particles in front of the swarming band will finally align with the band due to the anisotropic interaction. Actually, the specific setting of our model, wherein the active force acts opposite to the attractive interaction, also leads to a kind of repulsion-induced alignment. If the active force is zero, Janus particles attract each other and form small clusters with face-to-face configurations. If the active force is large enough, however, active force could pull the clusters apart and push the particles along the repulsive (back) side, such that the particles tends to be repulsive when they approach each other. Clearly, such a kind of repulsion-induced alignment would depend on the relative amplitude of the active force F_a and interaction strength C, making it is feasible to tune the swarming states in an efficient way.

To conclude, there is an emergence of swarming behaviors in the active Janus particle system when the directions of activity and anisotropic interaction are opposite. By tuning the activity and anisotropic interaction strength, we could control the collective states when area fraction exceeds the critical value. The mechanism of phase-separation of polar band is quite different from motility-induced phase separation. On one hand, for particles in front of the swarming band, anisotropic interactions make them aligning with the swarming direction, and the flux into the band increases with particle activity. On other hand, particles tend to drift out the band from the back surface, which is harder when the strength C of anisotropic interaction is larger.

These findings demonstrate the nontrivial roles of activity and anisotropic interaction. Commonly, the active Janus particles are synthesized by the Janus colloids coated with metal or amphiphilic polymer. The BAP model we propose provides a conceptually new approach to explore the collective behaviors of active Janus system. To synthesize the BAPs experimentally, we suggest a protocol in which an isotropic particle can be coated by two different layers of materials separately with the aimed biased angle, one of which produces anisotropic interaction and the other provides self-propulsion. Therefore we believe that the system of biased-active particles is worth further studying and has a variety of new fascinating collective behaviors that would open new perspectives for the design of smart active materials.

VI. ACKNOWLEDGMENTS

This work is supported by the Ministry of Science and Technology (2016YFA0400904 and 2018YFA0208702), the National Natural Foundation of China (No.21973085, No.21833007, No.21790350, No.21673212, No.21521001, and No.21473165), the Fundamental Research Funds for the Central Universities (No.WK2340000074), and Anhui Initiative in Quantum Information Technologies (No.AHY090200).

[1] S. N. Beshers and J. H. Fewell, Annu. Rev. Entomol. **46**, 413 (2001).
[2] J. Buhl, D. J. Sumpter, I. D. Couzin, J. J. Hale, E. Despland, E. R. Miller, and S. J. Simpson, Science **312**, 1402 (2006).
[3] J. E. Niven, Science **335**, 43 (2012).

[4] H. Wioland, E. Lushi, and R. E. Goldstein, New J. Phys. **18**, 075002 (2016).
[5] E. Lushi, H. Wioland, and R. E. Goldstein, Proc. Natl. Acad. Sci. USA **111**, 9733 (2014).
[6] J. Zhang, E. Luijten, B. A. Grzybowski, and S. Granick, Chem. Soc. Rev. **46**, 5551 (2017).
[7] M. K. Feng and Z. H. Hou, Chin. J. Chem. Phys. **31**, 584 (2018).
[8] T. Vicsek, A. Czirók, E. Ben-Jacob, I. Cohen, and O. Shochet, Phys. Rev. Lett. **75**, 1226 (1995).
[9] F. Farrell, M. C. Marchetti, D. Marenduzzo, and J. Tailleur, Phys. Rev. Lett. **108**, 248101 (2012).
[10] K. H. Nagai, Y. Sumino, R. Montagne, I. S. Aranson, and H. Chaté, Phys. Rev. Lett. **114**, 168001 (2015).
[11] R. Großmann, P. Romanczuk, M. Bär, and L. Schimansky-Geier, Phys. Rev. Lett. **113**, 258104 (2014).
[12] O. Chepizhko, E. G. Altmann, and F. Peruani, Phys. Rev. Lett. **110**, 238101 (2013).
[13] Y. Sumino, K. H. Nagai, Y. Shitaka, D. Tanaka, K. Yoshikawa, H. Chaté, and K. Oiwa, Nature **483**, 448 (2012).
[14] J. Yan, M. Han, J. Zhang, C. Xu, E. Luijten, and S. Granick, Nat. Mater. **15**, 1095 (2016).
[15] A. Bricard, J. B. Caussin, N. Desreumaux, O. Dauchot, and D. Bartolo, Nature **503**, 95 (2013).
[16] R. Dreyfus, J. Baudry, M. L. Roper, M. Fermigier, H. A. Stone, and J. Bibette, Nature **437**, 862 (2005).
[17] L. Baraban, M. Tasinkevych, M. Popescu, S. Sanchez, S. Dietrich, and O. Schmidt, Soft Matter **8**, 48 (2012).
[18] G. Volpe, I. Buttinoni, D. Vogt, H. J. Kümmerer, and C. Bechinger, Soft Matter **7**, 8810 (2011).
[19] D. A. Wilson, R. J. Nolte, and J. C. Van Hest, Nat.Chem. **4**, 268 (2012).
[20] W. Gao, A. Pei, X. Feng, C. Hennessy, and J. Wang, J. Am. Chem. Soc. **135**, 998 (2013).
[21] J. Li, O. E. Shklyaev, T. Li, W. Liu, H. Shum, I. Rozen, A. C. Balazs, and J. Wang, Nano Lett. **15**, 7077 (2015).
[22] J. Wang and W. Gao, ACS Nano **6**, 5745 (2012).
[23] H.-R. Jiang, N. Yoshinaga, and M. Sano, Phys. Rev. Lett. **105**, 268302 (2010).
[24] S. J. Ebbens and J. R. Howse, Langmuir **27**, 12293 (2011).
[25] R. F. Dong, Q. Zhang, W. Gao, A. Pei, and B. Ren, ACS Nano **10**, 839 (2016).
[26] H. Wang, G. Zhao, and M. Pumera, J. Am. Chem. Soc. **136**, 2719 (2014).
[27] A. Somoza, E. Chacón, L. Mederos, and P. Tarazona, J. Phys: Condens. Matter **7**, 5753 (1995).
[28] M. Pu, H. Jiang, and Z. Hou, Soft Matter **13**, 4112 (2017).
[29] S. A. Mallory, F. Alarcon, A. Cacciuto, and C. Valeriani, New J. Phys. **19**, 125014 (2017).
[30] Y. Gou, H. Jiang, and Z. Hou, Soft Matter **15**, 9104 (2019).
[31] J. D. Weeks, D. Chandler, and H. C. Andersen, J. Chem. Phys. **54**, 5237 (1971).
[32] G. Rosenthal, K. E. Gubbins, and S. H. Klapp, J. Chem. Phys. **136**, 174901 (2012).
[33] A. Nikoubashman, Soft Matter **13**, 222 (2017).
[34] M. E. Cates and J. Tailleur, Annu. Rev. Condens. Matter Phys. **6**, 219 (2015).
[35] G. S. Redner, M. F. Hagan, and A. Baskaran, Phys. Rev. Lett. **110**, 055701 (2013).
[36] Y. Fily, S. Henkes, and M. C. Marchetti, Soft Matter **10**, 2132 (2014).
[37] I. Buttinoni, J. Bialké, F. Kümmel, H. Löwen, C. Bechinger, and T. Speck, Phys. Rev. Lett. **110**, 238301 (2013).
[38] G. S. Redner, A. Baskaran, and M. F. Hagan, Phys. Rev. E **88**, 012305 (2013).
[39] S. D. Ryan, A. Sokolov, L. Berlyand, and I. S. Aranson, New J. Phys. **15**, 105021 (2013).
[40] J. J. Keya, R. Suzuki, A. M. R. Kabir, D. Inoue, H. Asanuma, K. Sada, H. Hess, A. Kuzuya, and A. Kakugo, Nat. Comm. **9**, 1 (2018).

DOI:10.1063/1674-0068/cjcp2003037